EPR of Eu^{2+} in $BaBr_2$ crystals and fluorobromozirconate glass ceramics

2001 J. Phys.: Condens. Matter 13 2331

(http://iopscience.iop.org/0953-8984/13/10/323)

INSTITUTE OF PHYSICS PUBLISHING JOURNAL OF PHYSICS: CONDENSED MATTER

J. Phys.: Condens. Matter **13** (2001) 2331–2338 www.iop.org/Journals/cm PII: S0953-8984(01)17987-7

EPR of Eu^{2+} in $BaBr_2$ crystals and fluorobromozirconate glass ceramics

S Schweizer[1], G Corradi[1,2], A Edgar[1,3] and J-M Spaeth[1]

[1] Department of Physics, University of Paderborn, D-33095 Paderborn, Germany
[2] Research Institute for Solid State Physics and Optics, Hungarian Academy of Sciences, Budapest, H-1525 Hungary
[3] School of Chemical and Physical Sciences, Victoria University, Wellington, New Zealand

Received 13 October 2000

Abstract

The x-ray storage phosphor properties of fluorozirconate glasses doped with Eu^{2+} and Br^- were interpreted previously to be due to $BaBr_2$:Eu^{2+} crystalline precipitates. In order to compare their behaviour with $BaBr_2$:Eu^{2+} single crystals, we grew such single crystals and investigated them with electron paramagnetic resonance (EPR). The Eu^{2+} EPR spectra show local C_S symmetry, with an isotropic g value 1.990 and an isotropic hyperfine constant $^{151}A = -31.0 \times 10^{-4}$. The principal axes of the zero field splitting tensor in the mirror plane are rotated by an angle of 18° with respect to the crystallographic axes, as expected for the Ba^{2+} site. A powder EPR spectrum was also recorded and successfully simulated using the single-crystal EPR data. Its close similarity with the EPR spectra in fluorobromozirconate glass ceramics doped with Eu^{2+} shows that indeed crystalline $BaBr_2$:Eu^{2+} precipitates are present in such glass ceramics.

1. Introduction

BaFBr:Eu^{2+}, the best-known x-ray storage phosphor so far, has been used for more than a decade in commercial imaging systems. The shortcomings of the presently used x-ray storage phosphor materials are a low spatial resolution (5 line pairs per mm) compared to the best x-ray films. The low resolution power is to a large extent the result of light scattering during the read-out process, since BaFBr:Eu^{2+} is birefringent and the BaFBr:Eu^{2+} crystallites in the screen have rather large scattering effects. One possible solution to this scattering problem would be a phosphor based on a glass. Indeed, there has been a recent report of the observation of photostimulable luminescence (PSL) in a fluorozirconate glass (with the ZBLAN formulation) doped with EuF_2 and NaBr [1]. X-ray diffraction showed that the Br^- doping caused the formation of crystalline $BaBr_2$ precipitates in the glass matrix. From electron paramagnetic resonance (EPR) it was assumed that Eu^{2+} was also incorporated into the precipitates, resulting in a characteristic Eu^{2+} powder EPR spectrum superimposed on the U-spectrum of Eu^{2+} ions in the glass matrix [2]. Since the glass did not show any PSL without Br^- doping, it was

0953-8984/01/102331+08$30.00

proposed that the PSL was due to the $BaBr_2$:Eu^{2+} precipitates. By x-ray diffraction (XRD) measurements the $BaBr_2$ precipitates were found to have the high-pressure anti-Fe_2P structure [1]. It was found later that depending on the annealing condition the precipitates can also be in the normal orthorhombic phase of $BaBr_2$ [3]. In this study we use those glass ceramics in which $BaBr_2$ is found in the normal orthorhombic phase.

It is known that orthorhombic $BaBr_2$:Eu^{2+} shows x-ray storage properties [4]. However, compared to BaFBr:Eu^{2+}, the PSL in $BaBr_2$:Eu^{2+} has the disadvantage of faster fading and seems therefore to be less attractive. Nothing is known about the fine-structure and the hyperfine interaction of the Eu^{2+} activator in $BaBr_2$. The aim of this investigation was, therefore, to study the EPR of the Eu^{2+} activator in $BaBr_2$ both in single crystals and powders, and to use the fine-structure and hyperfine data derived from single-crystal spectra for a simulation of a $BaBr_2$:Eu^{2+} powder spectrum. Comparison with the glass ceramic spectra should show then whether Eu^{2+} is incorporated in the crystalline precipitates of $BaBr_2$ or whether it occupies other sites such as aggregates or interfaces between the $BaBr_2$ precipitates and the glass matrix. The EPR spectra of Eu^{2+} in glass matrices are known from previous investigations [2]. They are almost independent of the particular glass, very broad and differ clearly from the spectra of Eu^{2+} in crystalline matrices.

2. Crystal structure

$BaBr_2$ crystallizes in the orthorhombic $PbCl_2$ structure with the lattice parameters $a = 8.276$ Å, $b = 4.956$ Å, and $c = 9.919$ Å [5]. Ba^{2+} ions occupy four crystallographically equivalent positions in the symmetry planes of the space group $D_{2h}^{16}(Pnma)$. Bromine ions also occupy two sets of such positions, giving eight anions in the unit cell.

Figure 1 shows an elementary cell containing four formula units of $BaBr_2$ projected on the *ab*, *bc*, and *ac* planes. The local symmetry of the cation sites where Eu^{2+} substitution is expected corresponds to the point group C_S with a single-symmetry plane parallel to the *ac* plane. The centre of the cell is a centre of inversion, which reduces the number of magnetically non-equivalent cation substitution sites to two. These are labelled 1 and 2 in figure 1. Sites of type 1 and 2 are related e.g. by glide mirror planes parallel to the *ab* or *bc* planes. The EPR angular dependence of a substitutional cation defect should accordingly contain only one set of lines for rotation of the magnetic field in the *ab* or *bc* planes, but two sets for all other orientations including all general directions in the *ac* plane. The same should hold for defects with displaced positions within the symmetry planes conserving C_S symmetry. For displaced positions outside the symmetry planes four magnetically inequivalent sites should be observed for general orientations but only two sets of lines for rotations in the *ab*, *bc*, and *ac* planes.

3. Experiment

The investigations were performed on Eu^{2+} doped fluorozirconate glasses (53% ZrF_4, 20% BaF_2, 20% NaF, 3% AlF_3, 1.5% LaF_3, 1.5% YF_3, and 1% EuF_2) and on Eu^{2+} and Br^- co-doped fluorozirconate glasses which were obtained by replacing most of the NaF by NaBr so that the total number of bromine ions was 5% of the total number of anions. The bromine co-doped glasses were crucible quenched to below the glass temperature of 260 °C [6], and annealed afterwards for times between 30 and 240 minutes at 275 °C. At these temperatures, the hexagonal 'high-pressure' phase which first forms converts to the orthorhombic phase as shown by XRD measurements [3]. The glass manufacture and the annealing procedure were carried out in an inert nitrogen atmosphere. There was also optical evidence for crystallization

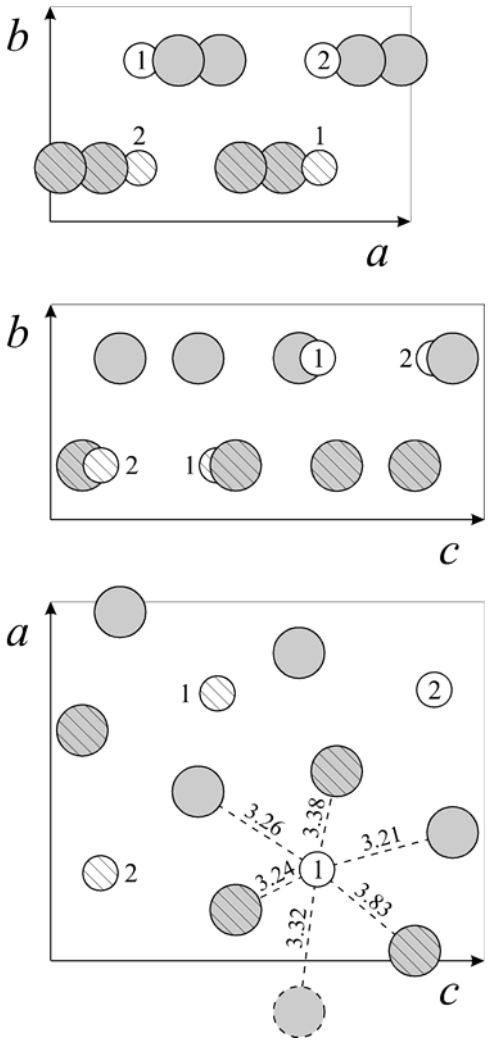

Figure 1. Lattice structure of orthorhombic $BaBr_2$ projected on the *ab*, *bc*, and *ac* planes, small white and large grey circles denoting Ba^{2+} and Br^{-} ions, respectively. The ions discerned by hatched circles lie in a different *ac*-type mirror plane than the non-hatched ones. Two types of magnetically non-equivalent Ba sites are labelled 1 and 2. The Ba–Br distances indicated are given in Å.

in the thermally treated glass, since the glasses showed a light yellow colour in transmitted light but blue in scattered light, as expected for a semi-transparent glass ceramic.

Single crystals of orthorhombic $BaBr_2$ were grown in the Paderborn crystal growth laboratory using the Bridgman method with a quartz glass ampoule, $SiBr_4$ atmosphere and $BaBr_2$ powder to which 1000 molar ppm of EuF_2 was added. The technique was modified for careful annealing and slow cooling through the cubic–orthorhombic transformation near 800 °C [7]. Prior to crystal growth the $BaBr_2$ powder was dried in vacuum with subsequent melting in $SiBr_4$ atmosphere to reduce oxygen contamination. The BaBr:Eu^{2+} single crystals were oriented using the Laue technique and cut to obtain samples with dimensions of a few millimetres along the main crystallographic directions. The powdered $BaBr_2$:Eu^{2+} samples were prepared by crushing pieces of the single crystal using a mortar and pestle. We have not yet been successful in producing single crystals of the hexagonal high-pressure phase.

The measurements were performed with a computer-controlled, custom-built x-band EPR/ENDOR spectrometer. The EPR spectra were evaluated with the 'Visual EPR' programme package using exact diagonalization procedures [8, 9].

4. Experimental results

4.1. EPR of single crystalline BaBr2:Eu2+

For a general direction of the magnetic field the EPR spectrum of Eu^{2+} in $BaBr_2$ essentially consists of two sets of seven fine-structure lines each (figure 2). Each of these lines has a hyperfine splitting of approximately 12 lines. Eu^{2+} has an $S = 7/2$ ground state and two stable isotopes: ^{151}Eu with $I = 5/2$ and 47.82% abundance and ^{153}Eu with $I = 5/2$ and 52.18% abundance. Each Eu isotope thus gives rise to a hyperfine structure of 6 lines; since the two nuclear g factors differ significantly so do the hyperfine interactions ($g_n(^{151}\text{Eu}) = 1.389$, $g_n(^{153}\text{Eu}) = 0.6134$), and consequently the two sextets are clearly resolved. This is in fact observed in figure 2 for several groups in both wings of the spectrum, additional lines in the central groups being due to 'forbidden' transitions with $\Delta m_I \neq 0$. This is in analogy with the case of Eu^{2+} in BaFBr [10, 11].

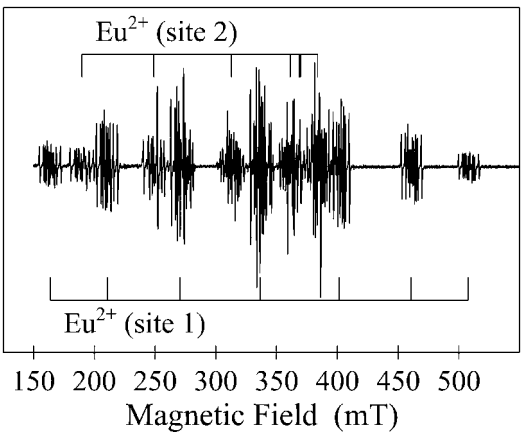

Figure 2. EPR spectrum of Eu^{2+} in a $BaBr_2$ single crystal for a general direction of the magnetic field $\vec{B}$ in the ac plane making an angle of 13° with the c direction, recorded at 20 K in x-band (9.37 GHz).

The EPR angular dependence of the Eu^{2+} fine-structure line positions determined as the centres of the hyperfine groups is shown in figure 3. The presence of only one set of lines in the ab and bc planes confirms that the dopant occupies sites of C_S local symmetry (see section 2). The angular dependence was analysed using a spin Hamiltonian of this symmetry with the ac plane as mirror plane. Since the ground state of Eu^{2+} is a pure S-state ($L = 0$), the g value and the hyperfine interaction are isotropic.

$$H = g\mu_b \vec{S}\cdot\vec{B} + \frac{1}{3}(b_2^0\hat{O}_2^0 + b_2^1\hat{O}_2^1 + b_2^2\hat{O}_2^2) + \frac{1}{60}(b_4^0\hat{O}_4^0 + b_4^1\hat{O}_4^1 + b_4^2\hat{O}_4^2 + b_4^3\hat{O}_4^3 + b_4^4\hat{O}_4^4) + \frac{1}{1260}(b_6^0\hat{O}_6^0 + b_6^1\hat{O}_6^1 + b_6^2\hat{O}_6^2 + b_6^3\hat{O}_6^3 + b_6^4\hat{O}_4^4 + b_6^5\hat{O}_4^5 + b_6^6\hat{O}_4^6) + A\cdot\vec{S}\cdot\vec{I} \quad (1)$$

where g is the isotropic g value, A the isotropic hyperfine constant of the ^{151}Eu or the ^{153}Eu isotope, the $\hat{O}_l^m$ are the Stevens operators and the b_l^m the Stevens parameters [12]. μ_B is the Bohr magneton and $\vec{S}$ is the electron spin operator. The obtained g and A values and the fine-structure parameters are collected in table 1 and were used for the calculation of the solid lines in figure 3. The EPR line positions yielded only relative signs for the fine-structure and hyperfine constants; the absolute signs have been derived from the intensity ratio between the highest field and lowest field hyperfine groups at low temperatures. Although the Stevens parameters b_6^m have to be included formally, they are not listed since they are zero within the error limits.

Table 1. g value, fine-structure and hyperfine parameters and their estimated errors for Eu^{2+} in $BaBr_2$. The fine-structure parameters b_k^q as well as the hyperfine value are given in units of 10^{-4} cm^{-1}. The main principal axis of the D tensor is in the ac plane and makes an angle of $(18 \pm 1)^\circ$ with the c-axis.

g	b_2^0	b_2^1	b_2^2	b_4^0	b_4^1	b_4^2	b_4^3	b_4^4	^{151}A
1.990	−237.7	−612.0	+123.2	+2.2	+24.0	+1.0	+23.3	+27.4	−31.0
±0.005	±1.0	±3.0	±1.0	±0.5	±1.0	±0.5	±3.0	±1.0	±0.5

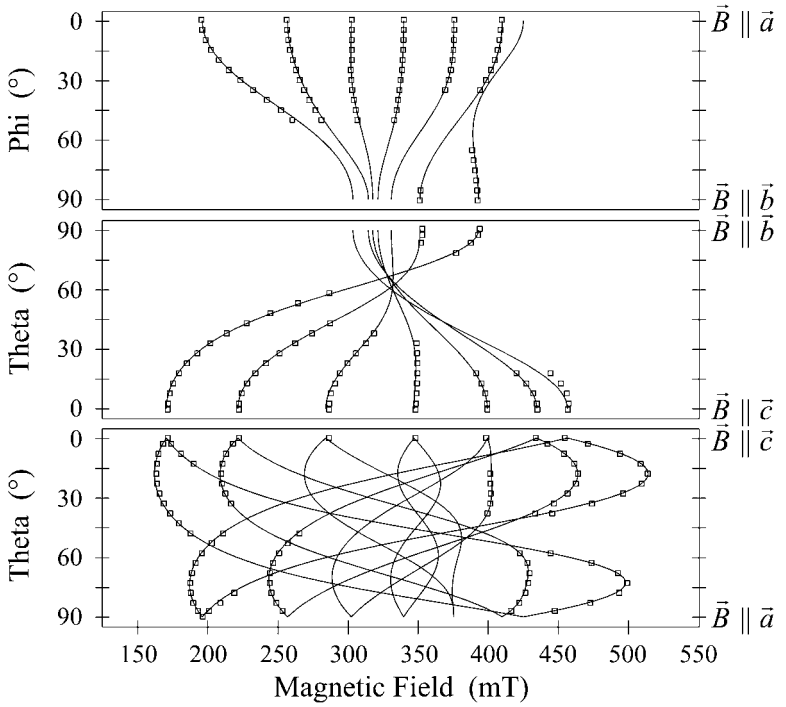

Figure 3. EPR angular dependence of the 'allowed' $\Delta m_s = \pm 1$ transitions of Eu^{2+} in $BaBr_2$ for a rotation of the magnetic field in the ab plane, in the bc plane and in the ac plane. The open squares represent the experimental positions of the fine-structure lines determined as centres of the Eu^{2+} hyperfine groups, the solid curves were calculated using the data in table 1. For the sake of clarity the Eu^{2+} hyperfine interaction is not shown.

The hyperfine splitting due to ^{151}Eu could be fitted for all orientations assuming an isotropic interaction Hamiltonian with $^{151}A = -(31.0 \pm 0.5) \times 10^{-4}$ cm^{-1}. For the ^{153}Eu isotope a similar constant scaled down by the nuclear g-factor ratio can be used, a possible small deviation from this proportionality [13] should be limited by the experimental error.

In addition to the mentioned $\Delta m_I \neq 0$ lines inside the central groups, some additional small features outside the groups have also been observed. As shown by simulation using the data of table 1 these correspond to EPR transitions with $|\Delta m_S| > 1$. Their presence, in particular in the low-field region below 150 mT where no other lines show up, is crucial for the explanation of the powder spectrum.

4.2. EPR of Eu^{2+} doped ZBLAN glass ceramics and powdered $BaBr_2$:Eu^{2+}

Figure 4, curves (a) and (b) show the EPR spectra of a Eu^{2+} doped crystal-free ZBLAN base glass and a Eu^{2+} and Br^- co-doped ZBLAN glass ceramic, respectively. In figure 4(b) the so-called ubiquitous or U-spectrum of Eu^{2+} in the ZBLAN base glass (figure 4(a)) [2] is superimposed by an additional EPR spectrum, whose structure is very similar to the powder EPR spectrum of $BaBr_2$:Eu^{2+} (figure 5(a)). Note, that the U-spectrum of the ZBLAN base glass differs only slightly from the U-spectrum in the ZBLAN glass ceramic.

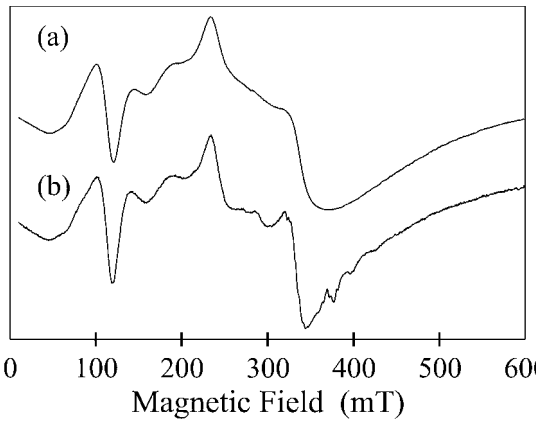

Figure 4. EPR of (a) Eu^{2+} doped ZBLAN and (b) Eu^{2+} and Br^- co-doped ZBLAN. The spectra were recorded at 20 K in x-band (9.29 GHz).

In figure 5(a) and 5(b) we show the observed and computed powder EPR spectra for europium-doped barium bromide. The spectrum in figure 5(b) was obtained by averaging 3200 single-crystal spectra simulated for orientations smoothly distributed on the surface of a sphere, using a linewidth of 1.5 mT and the parameters given in table 1. The linewidth is larger than the experimental linewidth of (0.5 ± 0.1) mT for single crystals, and was found to give a slightly better overall agreement than the experimental one. This is apparently due to the roughness of the grid chosen, which was inevitable as the computer time needed for 3200 orientations was already several days. The calculated spectrum in figure 5(b) shows very good agreement reproducing all major features and also most details of the experimental powder spectrum in $BaBr_2$:Eu^{2+} (figure 5(a)). A minor difference in the simulated spectrum is the nearly vanishing intensity of the 'forbidden' transitions ($|\Delta m_S| > 1$) in the magnetic field range below 150 mT.

5. Discussion

As shown by the qualitative analysis, the Eu^{2+} centre in $BaBr_2$ single crystals has C_S symmetry. The ground state of Eu^{2+} is a pure S-state ($L = 0$) with an isotropic g value very close to the g_e value of the free electron. The observed splitting of the S-state (fine structure) is due to higher-order effects of the crystal field and spin–spin interaction at the Eu^{2+} site. For the analysis of the zero field splitting it is useful to express the Stevens parameters b_2^m by

$$\underline{\underline{D}} \begin{pmatrix} \frac{1}{3}(-b_2^0 + b_2^2) & 0 & \frac{1}{6}b_2^1 \\ 0 & \frac{1}{3}(-b_2^0 - b_2^2) & 0 \\ \frac{1}{6}b_2^1 & 0 & \frac{2}{3}b_2^0 \end{pmatrix} \tag{2}$$

where $\underline{\underline{D}}$ is the fine-structure tensor D. The principal axes system of the D tensor can be obtained from the crystallographic system abc by a single rotation around the b-axis which is one of the principal axes, the other two lying in the ac-type mirror plane. The rotation angle is found to be

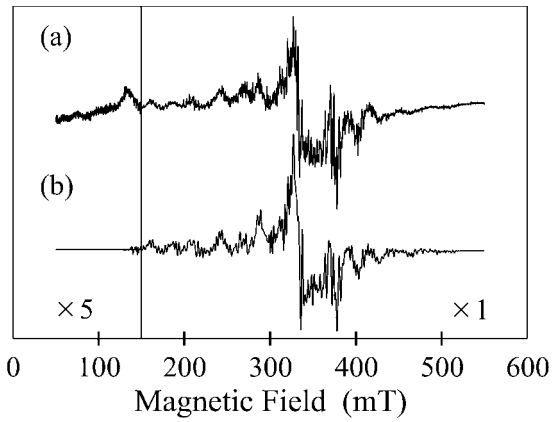

Figure 5. (a) EPR on powdered $BaBr_2$:Eu^{2+}, recorded at 20 K in x-band (9.33 GHz). (b) Calculated powder EPR spectrum of $BaBr_2$:Eu^{2+}, using a linewidth of 1.5 mT and the spin Hamiltonian parameters of table 1. The magnetic field range below 150 mT is scaled up in favour of the 'forbidden' transitions.

$(18 \pm 1)^\circ$ and the principal values are +153.6, +38.2, and −191.8 in units of 10^{-4} cm^{-1}. The crystal field at the Eu^{2+} site is mainly determined by nine surrounding Br^- ions. The Ba site has its nearest Br neighbour at 3.21 Å, situated in the same mirror plane, and the next two Br neighbours at 3.24 Å in the layers above and below (see figure 1). For the nearest neighbour the Ba–Br direction makes an angle of 15.3° with the *c* direction, while for the *ac*-plane projection of the next two Ba–Br directions this angle is 26.7°. These three neighbours apparently play a decisive role in defining the main principal axis of the *D* tensor. This is a strong argument for Eu^{2+} to be substituted at the Ba^{2+} site with essentially no displacement from the site.

The value found for the isotropic ^{151}Eu hyperfine interaction constant has the same sign and is in the same range as the ^{151}A values found in similar matrices (see e.g. [10, 13]). This is not surprising since the unpaired 4f orbital and its overlap with the 5s orbitals within the Eu^{2+} ion core, mediating the hyperfine interaction to the nucleus, is rather independent of the orbitals of the neighbouring atoms.

The powder EPR spectrum of $BaBr_2$:Eu^{2+} can be simulated successfully using our single-crystal data (figure 5). Comparison of the simulated powder EPR spectrum with the EPR spectrum in ZBLAN glass ceramic doped with Eu^{2+} and Br^- yields a qualitative agreement: the main features of the additional EPR spectrum attributed to Eu^{2+} in $BaBr_2$ precipitates (orthorhombic phase) in the glass ceramic such as its main maxima and minima are reproduced well (figure 6(a) and 6(b)). The Eu^{2+} hyperfine interaction has been omitted in the simulated spectrum of figure 6(b) since it causes only a substructure of the main maxima and minima discussed here. The separations between these maxima and minima depend mainly on the zero field splitting. For example, the increase of the zero field splitting (fine structure parameter b_2^0) by only 20% is clearly seen in the corresponding powder EPR spectrum (figure 6(c)) as a significant shift of the maxima and minima, particularly at low and high fields. Since b_2^0 is very sensitive to the crystalline environment of Eu^{2+} which has been shown in detail by [10], our analysis confirms that Eu^{2+} is incorporated in the crystalline precipitates of $BaBr_2$. Eu^{2+} does not occupy other sites such as aggregates or interfaces between the $BaBr_2$ precipitates and the glass matrix. The powder spectrum of BaBr:Eu^{2+} has sharper features indicating that in ZBLAN the inclusion of the crystallites into the glassy environment causes some deviations of the spin Hamiltonian parameters. An investigation of the distribution of precipitate sizes

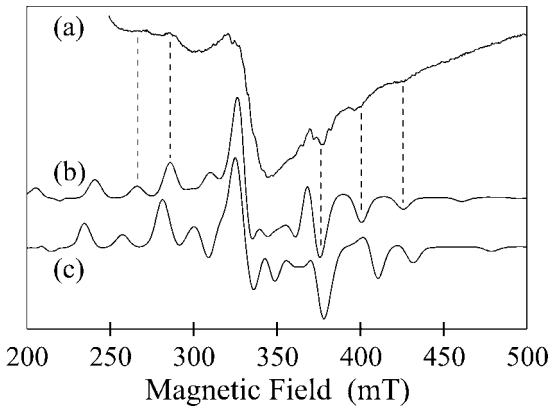

Figure 6. (a) Fraction of the EPR spectrum of Eu^{2+} and Br^{-} co-doped ZBLAN, recorded at 20 K in x-band (9.29 GHz). (b) Calculated powder EPR spectrum of $BaBr_2$:Eu^{2+}, using a linewidth of 7.5 mT and the spin Hamiltonian parameters of table 1. The Eu^{2+} hyperfine interaction has been omitted (see text). (c) Calculated powder EPR spectrum as for (b) but with a 20% larger fine structure parameter b_2^0.

and possible grain size effects in EPR would be of interest, together with the production and study of the high-pressure phase in single-crystal form.

Acknowledgments

One of the authors (GC) would like to thank the Hungarian Scientific Research Fund (OTKA T34262).

References

[1] Edgar A, Spaeth J-M, Schweizer S, Assmann S, Newman P J and Macfarlane D R 1999 *Appl. Phys. Lett.* **75** 2386
[2] Furniss D, Harris E A and Hollis D B 1987 *J. Phys. C: Solid State Phys.* **20** L147
[3] Edgar A 2000 private communication
[4] Iwase N, Tadaki S, Hidaka S and Koshino N 1994 *J. Lumin.* **60–61** 618
[5] Brackett E B, Brackett T E and Sass R L 1963 *J. Phys. Chem.* **67** 2132
[6] Ohsawa K and Shibata T 1984 *J. Lightwave Technol.* **LT-2** 602
[7] Monberg E and Ebisuzaki Y 1973 *J. Cryst. Growth* 307
[8] Grachev V G 1987 *JETP* **92** 1834
[9] Grachev V G 1993 *G-symmetry and theory of ENDOR frequencies of centers with low-symmetry interaction: Radiospectroscopy of Solid State* (Kiev: Naukova Dumka) pp 16–66
[10] Nicollin D and Bill H 1978 *J. Phys. C: Solid State Phys.* **11** 4803
[11] Assmann S, Schweizer S and Spaeth J-M 1999 *Phys. Status Solidi* (b) **212** 325
[12] Stevens K W H 1952 *Proc. Phys. Soc.* **65** 209
[13] Abragam A and Bleaney B 1970 *Electron paramagnetic resonance of transition ions* (New York: Oxford University Press)